GEOFIZIKA VOL. 33 2016

DOI: 10.15233/gfz.2016.33.11
Original scientific paper
UDC 550.34.01

Modeling shear stress distribution in natural small streams by soft computing methods

Onur Genc [1], Ozgur Kisi [2] and Mehmet Ardiclioglu [3]

[1] Meliksah University, Department of Civil Engineering, Kayseri, Turkey

[2] International Black Sea University, Center for Interdisciplinary Research, Tbilisi, Georgia,

[3] Erciyes University, Department of Civil Engineering, Kayseri, Turkey

Received 3 April 2016, in final form 10 October 2016

In this study, artificial neural networks (ANNs) and adaptive neuro-fuzzy inference system (ANFIS) were used to estimate shear stress distribution in streams. The methods were applied to the 145 field data gauged from four different sites on the Sarimsakli and Sosun streams in Turkey. The accuracy of the applied models was compared with the multiple-linear regression (MLR). The results showed that the ANNs and ANFIS models performed better than the MLR model in modeling shear stress distribution. The root mean square errors (*RMSE*) and mean absolute errors (*MAE*) of the MLR model were reduced by 47% and 50% using ANFIS model in estimating shear stress distribution in the test period, respectively. It is found that the best ANFIS model with *RMSE* of 3.85, *MAE* of 2.85 and determination coefficient (R^2) of 0.921 in test period is superior to the MLR model with *RMSE* of 7.30, *MAE* of 5.75 and R^2 of 0.794 in estimation of shear stress distribution, respectively.

Keywords: ANN, ANFIS, linear regression, shear stress, stream, turbulent flow

1. Introduction

Stream flow is still a study area today for researchers who want to explore the complex characters of stream flows. The shear stress distribution is the one of these properties to be investigated. The particles of the fluid have different velocities. The velocity of the particle will vary from layer to layer as its distance varies from the boundary in open channel flow. The shear stress is the force per unit area in the flow direction. Shear stress in streams cannot be determined directly but is predicted using measurements of flow velocity or flow properties and their relation with the shear stress. The transverse distribution of shear stress in streams is known to be affected by the geometry of the cross section, the boundary roughness distribution and the structure of secondary flows (Ghosh and Roy, 1970; Knight and Patel, 1985; Yang and Lim, 2005).

Determination of shear stress distribution in streams is important not only for the design of water resources but also for the definition of structure of the turbulent flow in streams. Although many researchers have already investigated for solution of the problem, the shear stress distribution in streams cannot be still fully understood. The importance of determination of transverse shear stress distribution is stressed by the use of local or average shear stress in many hydraulic equations concerning the computation of flow resistance, sidewall correction, sediment transport rate, channel erosion or deposition, and design of channels. Currently, the mean bed and side wall shear stresses are used to designing and modeling river due to the shortage of knowledge of the transverse distribution of shear stress. These approaches are not an economical and reliable (Hicks et al., 1990).

After the measurements on secondary flows have been started, investigations on the shear stress distribution accelerated. An analytical method was improved to determine the bottom shear stress in a shallow, symmetrical channel by Lundgren and Johnson (1960). Shear stress distributions in open channel flows have been investigated by a number of authors (Tracy, 1965; Knight et al., 1994; Zheng and Jin, 1998; Ardiclioglu et al., 2006). Knight et al. (1984) improved an empirical equation which gives the percentage of the total shear force as given in the following form

$$\log(\%SF_w) = -1.4026 \times \log\left(\frac{B}{H} + 3\right) + 2.6692 \tag{1}$$

where B is the breadth of the channel and H is the depth of flow.

Then, Knight and Patel (1985) performed a series of experiments for rectangular duct flume and presented Eq. (2)

$$\%SF_w = \frac{103.23}{\left(1 + \frac{2b}{3h}\right)^{1.4128}} \tag{2}$$

where b is the width of duct and h is the height of duct.

Determination of the local or average shear stress as sensitive is a quite difficult study even using advanced turbulence models. Empirical, analytical or simplified approaches were presented to calculate shear stress distribution by many investigators such as Christensen and Fredsoe (1998), Berlamont et al. (2003). The distribution of shear stress in a V-shaped channel was investigated by Mohammadi and Knight (2004). The distribution of boundary shear stress along the wetted perimeter in two dimensional flows was obtained using flow-net by Yu and Tan (2007). Distribution of boundary shear stress and the average bed and wall shear stresses in prismatic open channel flows were calculated using six

different methods and the results were compared by Khodashenas et al. (2008). Cacqueray et al. (2009) investigated the shear stress in smooth rectangular channels using detailed Computational Fluid Dynamics (CFD) simulation results. They showed that their CFD simulations are consistent. All of these investigations on secondary flows and shear stress distributions performed by researchers have showed that it is necessary and significant a simple, practical model to understand the shear stress distribution in streams.

Ardiclioglu et al. (2012) stressed that one dimensional hydraulic equations was used to explain the flow in open channels. Because of river hydrodynamics is quite complicated, these hydraulic equations are insufficient to determine the flow properties. Recently, artificial neural networks (ANNs) and adaptive neuro-fuzzy inference system (ANFIS) techniques have been successfully used to solve problems of the water resources and hydraulic engineering. Yang and Chang (2005) used ANN for simulation of velocity profiles, velocity contours and discharges. Kocabas and Ülker (2006) modeled critical submergence for an intake in a stratified fluid media by using ANFIS. Dogan et al. (2007) estimated sediment concentration obtained by experimental study by ANN method. Cobaner et al. (2008) used ANN for modeling bridge backwater. Mamak et al. (2009) used both ANN and ANFIS models for analyzing bridge afflux through arched bridge constrictions. Riahi-Madvar et al. (2009) predicted longitudinal dispersion coefficient in natural streams by using ANFIS. Kocabas et al. (2009) predicted critical submergence by using ANN.

Cobaner et al. (2010) developed an ANN model to estimate the boundary shear stress distributions in smooth rectangular channels and ducts. They used 94 experimental data obtained from the studies of well-known researchers in this field. According to result of this study, the ANN model performed slightly better than the classical methods. Bilhan et al. (2010) used two different ANN techniques for modeling lateral outflow over rectangular side weirs. Guven (2011) modeled scour geometry downstream from hydraulic structures by using ANN. Dursun et al. (2012) estimated discharge coefficient of semi-elliptical side weir using ANFIS. Can et al. (2012) modelled the daily streamflow using autoregressive moving average (ARMA) and ANNs in Çoruh Basin in Turkey. They selected nine gauging stations that are operated by Turkish General Directorate of Electrical Power Resources and Development Administration (EIE). Their study revealed that the historical time series have similar statistical parameters to those of the generated time series at 95% confidence level. Kisi et al. (2013) used ANFIS approach and successfully modeled the discharge capacity of rectangular side weirs. Marsili-Libelli et al. (2013) proposed a new stream flow assessment method based on fuzzy habitat suitability and large scale river modeling. Wolfs and Willems (2013) used ANFIS for computationally efficient lumped floodplain modeling. Rezaeianzadeh et al. (2013) investigated flood flow forecasting using ANN, ANFIS and regression models. They showed that nonlinear regression can be applied as a quick method for predicting the maximum daily

flow. Tayfur et al. (2014) estimated hydraulic conductivity in heterogeneous aquifers by using ANN and ANFIS methods. Baghari et al. (2014) used ANN method in order to identify the most important parameters affecting the discharge coefficient of rectangular sharp-crested side weirs.

In this paper, the applicability of the ANN and ANFIS approaches for modeling shear stress distributions on natural streams is investigated. The results are compared with the multiple-linear regression model.

2. Field measurements

Recent studies of flow measurements on Kızılırmak and Seyhan Basins in Central Turkey have broaden understanding of flow properties in the Kızılırmak and Zamantı River. Twentytwo (22) measurement studies were performed at four different stations on Kızılırmak and Seyhan Basins by a team that consists of first and third authors. The names of measured stations are Barsama, Bünyan, Şahsenem and Sosun. Sosun Station where is in Seyhan basin and tributary of Zamantı River was visited between 2009 and 2010. The Zamantı River which is one of the branches of the Seyhan River originates in Pınarbaşı, Kayseri and drains into the Mediterranean Sea in southern Turkey. Measurement studies on Barsama, Şahsenem and Bünyan Stations where are in Kızılırmak Basin and at tributary of Kızılırmak River was carried out between 2005 and 2010. Kızılırmak basin is the second biggest basin in Turkey. Kızılırmak is the longest river that originates in Sivas and drains into the Black Sea in northern Turkey (Fig. 1). In Fig. 2, measurements at Barsama and Şahsenem stations are given.

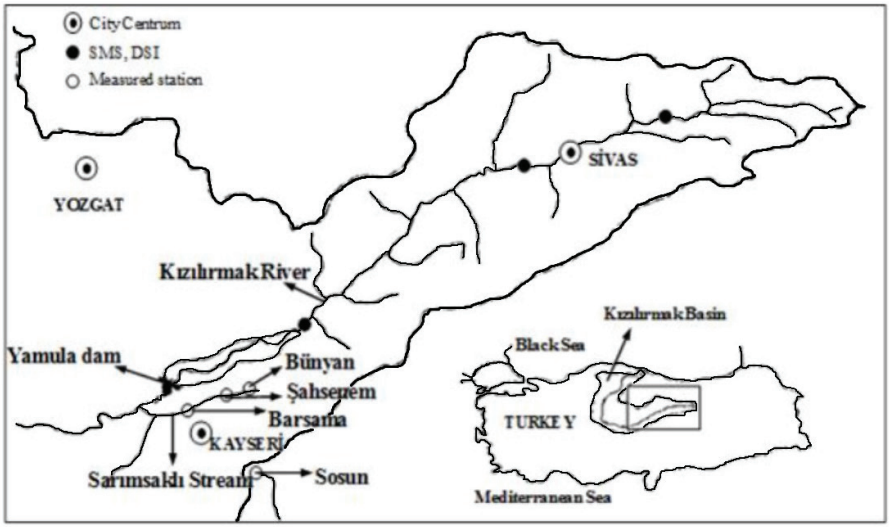

Figure 1. Location of the study area and measurement stations at Bünyan, Şahsenem, Barsama and Sosun (Ardiclioglu et al., 2012).

Figure 2. Velocity and topographical measurements at (*a*) Barsama and (*b*) Şahsenem Stations (Ardicliogl u et al. 2012).

The technology of flow measurement devices has evolved rapidly in recent decades. Many flow measuring devices were discovered to determine the flow properties. The Acoustic Doppler velocimeter, ADV which is one of these devices was utilized to measure three dimensional velocity data at the measured stations. The ADV is used to measure water velocity in a wide range of environments including laboratories, rivers, estuaries, and the ocean. An ADV operates by the principle of Doppler shift. All ADV measures the velocity samples by sending out short acoustic waves from the transmitter probe. These waves travel to moving particulates in the liquid and three receiving probes record for the change in frequency of the returned waves. The velocity vector is transmitted to recorder of ADV. Three-dimensional flow velocities (u, v, w) for x, y, z directions can be measured by ADV in a sampling volume. Furthermore, ADV can be used to record one second velocity data for the specified averaging time, location, and water depth parameters (to document the data set), and a variety of statistical and quality control data. The ADV can measure sampling volume from 10 cm front of the probe head. Thus, the probe head itself does not much impact on the flow field surrounding the measurement volume. Velocity range is between ±0.001 m/s and 4.5 m/s, resolution 0.0001 m/s, accuracy ±1% of measured velocity (Sontek, 2002).

According to the water surface width (T), the stream is divided into segments for each field measurements. As seen in Tab. 1, wide channels ($T/R \geq 10$) have 7–10 slices and narrow channels ($T/R < 10$) have 4–7 slices. Point velocity is measured by ADV and cross-section area is measured using depth data measurements of distances from a fixed reference point on the riverbank. Point velocities were measured in the vertical direction starting 4 cm from the streambed for each vertical. Point velocity values were measured in the vertical direction starting 4 cm from the streambed for each vertical. Measurements were repeated every 2 cm from this point to water surface. The velocities of free water surface in all verticals were estimated using extrapolating the last two measurements of verticals. And also mean water surface velocities (u_{ws}) were measured at each visited stations. Water surface velocities were measured by how many seconds a tree branch passed distance of 10 meters using a chronometer. These measurements were repeated 10–15 times. In this way, we determined the average u_{ws} for all flow conditions and stations and given in the column 4 of Tab. 1.

The flow characteristics at each site are summarized in Tab. 1. As shown in Tab. 1, six measurements have been made at Barsama, Şahsenem and Bünyan stations in 2005–2006. Also, four measurement studies were undertaken at Sosun Station in 2009–2010.

The flow characteristics at each site are given in Tab. 1. In this table, first and second columns show visit numbers and dates of stations, U_m (= Q / A) is the mean velocity, u_{ws} is the measured water surface velocity, with A being the area of the cross section, H_{max} is the maximum flow depth, and T/R is the aspect ratio, with T being the surface water width, R (= A/P) is the hydraulic radius, P is

wetted perimeter. Re ($= 4\,U_m\,R/v$) is the Reynolds number, and v is the kinematic viscosity, Fr ($= U_m/(g\,H_{max})^{1/2}$) is the Froude number, where g is the gravitational acceleration, and S is water surface slope. According to the Froude and Reynolds numbers all the flow measurements are under subcritical and turbulent flow conditions according to Froude and Reynolds numbers. Froude numbers are between 0.084–0.578, aspect ratios (T/R) vary between values 6.53–45.40. Reynolds numbers ($Re \times 10^6$) vary between 0.32–1.47.

Table 1. Flow characteristics for all stations.

Stations	Dates (dd/mm/year)	U_m (m/s)	u_{ws} (m/s)	H_{max} (m)	T (m)	T/R	Re ($\times 10^6$)	Fr	S
Barsama_1	28/05/2005	0.890	1.60	39.0	8.3	34.00	0.76	0.481	0.0091
Barsama_2	19/05/2006	1.051	1.85	40.0	9.0	35.20	0.94	0.531	0.0036
Barsama_3	19/05/2009	1.214	2.08	45.0	9.0	29.70	1.47	0.578	0.0094
Barsama_4	31/05/2009	0.590	1.14	26.0	8.4	45.40	0.40	0.333	0.0092
Barsama_5	24/03/2010	0.806	1.55	38.0	8.6	34.40	0.61	0.417	0.0097
Barsama_6	18/04/2010	0.865	1.63	38.2	8.8	22.10	0.85	0.421	0.0120
Bünyan_1	24/06/2009	0.354	0.65	72.0	4.0	7.00	0.71	0.133	0.0020
Bünyan_2	08/02/2010	0.214	0.40	66.0	4.0	7.50	0.40	0.084	0.0030
Bünyan_3	27/09/2009	0.301	0.54	72.0	3.9	8.20	0.50	0.113	0.0022
Bünyan_4	04/04/2010	0.405	0.74	85.0	4.0	7.30	0.78	0.140	0.0018
Bünyan_5	16/05/2010	0.426	0.54	86.0	4.0	7.00	0.85	0.147	0,0024
Bünyan_6	20/06/2010	0.286	0.53	79.0	3.9	7.30	0.53	0.103	0.0010
Şahsenem_1	29/03/2006	0.600	1.04	28.0	6.0	26.80	0.47	0.350	0.0059
Şahsenem_2	20/10/2007	0.529	0.93	32.0	5.4	21.90	0.46	0.298	0.0061
Şahsenem_3	22/03/2008	0.565	0.80	33.0	6.0	22.10	0.49	0,314	0,0037
Şahsenem_4	03/05/2008	0.518	1.00	32.0	5.4	25.10	0.39	0.307	0.0045
Şahsenem_5	11/10/2008	0.536	1.01	32.0	5.5	22.00	0.44	0.303	0.0046
Şahsenem_6	08/11/2008	0.516	1.00	34.0	5.6	19.60	0.51	0.282	0.0064
Sosun_1	19/05/2009	0.561	0.96	62.0	3.2	7.49	0.84	0.227	0.0032
Sosun_2	31/05/2009	0.285	0,63	43.0	3.0	9,49	0.32	0.144	0.0016
Sosun_3	24/03/2010	0.327	0.63	45.0	2.9	8.85	0.37	0.156	0.0026
Sosun_4	18/04/2010	0.541	0.93	54.0	2.3	6.53	0.67	0.235	0.0034

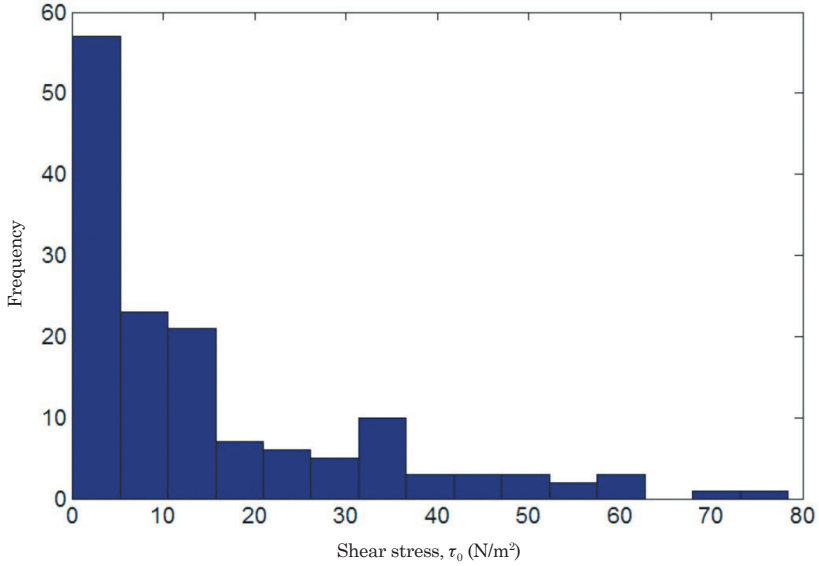

Figure 3. The frequency histograms of the target variable, shear stress τ_0.

Figure 3 presents the scatter plots for frequency histogram of 145 shear stress, τ_0 values in measured vertical. As seen from the figure, the most of shear stress, τ_0 values change between the values 0–20 N/m^2. The minimum shear stress is 0.081 N/m^2 and the maximum shear stress is 78.4 N/m^2.

3. Shear stress distributions

Shear stress distribution basically depends upon the geometry of the cross section and the mechanism of the secondary flow cells. Shear force in uniform flow can be defined as in below

$$F_t = \gamma A L S \tag{3}$$

where γ is the specific weight or unit weight of water, A is the channel cross sectional area, L is the length of the control volume and S is the longitudinal slope of the channel. Unit shear force is calculated using Eq. (3) as following form.

$$\tau_0 = \frac{\gamma ALS}{PL} = \gamma RS \tag{4}$$

where, τ_0 is the average value of the shear force per unit of the wetted area, R is the hydraulic radius (= A / P in which A is the wetted area and P is wetted perimeter).

It is clear that, shear force is not always uniformly distributed over the perimeter. French (1985) stressed that for a sensitive calculation methodology to be determined, the distribution of the shear force on the perimeter of the channel should be predicted.

Schlicting (1987) informed that logarithmic relation between the shear velocity and the variation of velocity with height is used to determine the local bed shear stress.

$$\frac{u}{u_*} = \frac{1}{\chi} \ln\left(\frac{z}{k_s / 30}\right) \tag{5}$$

where u is stream wise velocity at z, $u_* = (\tau_0/\rho)^{1/2}$ is the shear velocity, ρ is water density, k_s is the Nikuradse's original uniform sand grain roughness, χ is the von Kármán constant and z is distance from the bottom of the roughness elements.

4. Method

4.1. Artificial neural networks

ANNs are developed by getting inspired from real nervous system by neglecting most of the biological details. They are massively parallel systems consisting many processing elements, called neurons. Each layer in ANNs is fully connected to the proceeding layer by interconnection weights. Figure 4 represents a three layered ANN comprising layers i, j, and k, with the weights W_{ij} and W_{jk} between layers. Initial weight values are randomly assigned and then corrected during a training process. This process compares model outputs with measured outputs and back propagates any errors (from right to left in Fig. 4). Thus, the final weights are obtained by minimizing the errors (Kisi, 2005).

In layers j and k, each neuron receives the x input which is the weighted sum of outputs from the previous layer. As an example, in layer j, y can be given as

$$y_{pj} = \sum_{i=1}^{I} W_{ij} O_{pi} + \theta_j \tag{6}$$

in which θ_j is a bias for neuron j, O_{pi} is ith output of the previous layer, W_{ij} is the weights between the layers i and j. An output $f(y)$ is obtained from each neuron in layers j and k by passing y value through a non-linear activation function. Logistic function is commonly used as an activation function

$$f(y) = \frac{1}{1 + e^{-y}} \tag{7}$$

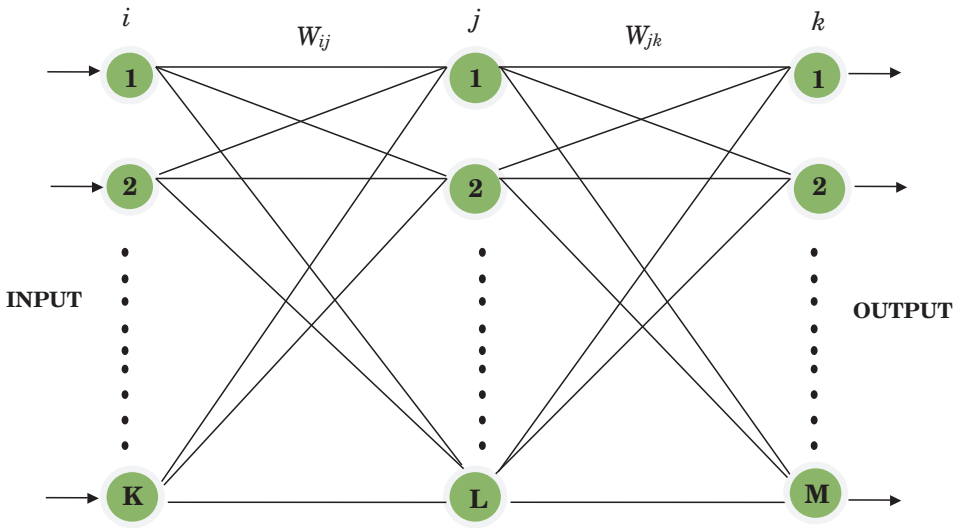

Figure 4. A three-layered ANN structure (Kisi, 2005).

The detailed theoretical information about ANNs can be obtained from the related references (Haykin, 2009).

4.2. Adaptive neuro-fuzzy inference system

ANFIS is first pioneered by Jang (1993). As a universal approximator, it is capable of approximating any real continuous function. The structure of ANFIS is illustrated in Fig. 5. As also seen from the figure that its structure is composed of a number of nodes connected through directional links and each node has a function consists of fixed or adjustable parameters (Jang, 1997).

Assume a fuzzy inference system having three x, y and z inputs and one f output and its rule base consist of two Takagi and Sugeno fuzzy IF-THEN rules

Rule 1: IF x is A_1, y is B_1 and z is C_1 THEN

$$f_1 = p_1 x + q_1 y + r_1 z + t_1 \tag{8}$$

Rule 2: IF x is A_2, y is B_2 and z is C_2 THEN

$$f_2 = p_2 x + q_2 y + r_2 z + t_2 \tag{9}$$

in which f_1 and f_2 respectively refer to the output function of rule 1 and rule 2.

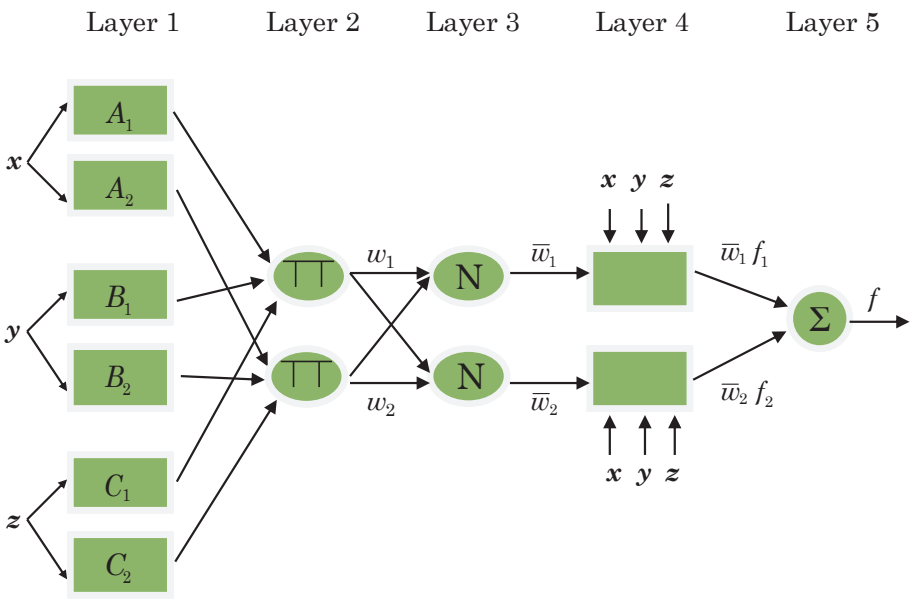

Figure 5. The structure of an ANFIS.

Every node i in layer *1* includes an adaptive node function

$$O_{l,i} = \varphi A_i(x) \text{ , for i = 1, 2} \tag{10}$$

where x is the ith node's input and A_i is a linguistic label such as "small" or "big" associated with this node function. $O_{l,i}$ refers the membership function of a fuzzy set A (in this example; A_1, A_2, B_1, B_2, C_1, or C_2). It denotes the degree to which the given input x satisfies the A_i. Gaussian function is usually chosen for the $\varphi A_i(x)$

$$\varphi A_i(x) = \exp\left(-\left(\frac{x-a_i}{b_i}\right)^2\right) \tag{11}$$

where a_i and b_i are the function's parameters. When the values of these parameters change, the Gaussian function also varies accordingly, thus various forms of membership functions are exhibited on linguistic label A_i (Jang, 1993). The parameters in this layer are named as premise parameters.

In layer 2, the incoming signals are multiplied in each node. For instance,

$$w_i = \varphi A_i(x)\varphi B_i(y)\varphi C_i(z) \text{ , i = 1, 2.} \tag{12}$$

The output of each node indicates the firing strength of a rule.

In layer 3, the ratio of the *i*th rule's firing strength to the sum of all rules' firing strengths is obtained by *i*th node as

$$\bar{w}_i = \frac{w_i}{w_1 + w_2}, \text{ i} = 1, 2. \tag{13}$$

In layer 4, each node has a function given in Eq. 14

$$O_{4,i} = \bar{w}_i f_i = \bar{w}_i (p_i x + q_i y + r_i z + t_i) \tag{14}$$

in which $\bar{w}_i$ is the output of layer 3, and p_i, q_i, r_i and t_i are the consequent parameters.

In layer 5, the final output is computed as the summation of all incoming signals

$$O_{5,i} = \sum \bar{w}_i f_i = \frac{\sum_i w_i f_i}{\sum_i w_i} \tag{15}$$

Thus, the ANFIS network which is functionally equivalent to a first-order Sugeno fuzzy inference system has been constructed. Detailed information for ANFIS, the readers are referred to the related references (Jang, 1993).

5. Results and discussion

In the current study, two different program codes including MATLAB neural network and fuzzy toolboxes were prepared for simulation of ANN and ANFIS models. Water surface velocity u_{ws}, water surface slope S and y/T were used as inputs to the models to estimate shear stress distribution. One hundred forty five (145) field measured data were used in development of the ANN, ANFIS and MLR models. After randomly permutation, whole data were divided into training and testing parts. The first data set (116 values, 80% of the whole data) was used for training and the obtained models were tested using the second data set (29 values, 20% of the whole data). Before applying ANN to the data set, the training input and output values were normalized between 0.2 and 0.8 by using the following equation

$$c_1 \frac{x_i - x_{\min}}{x_{\max} - x_{\min}} + c_2 \tag{16}$$

in which x_{max} and x_{min} refer to maximum and minimum of the training/test data. Here, the c_1 and c_2 values were respectively assigned as 0.6 and 0.2. The optimal

ANN models were obtained after trying various model structures. The evaluating criteria used in the study are root mean square errors (*RMSE*), mean absolute errors (*MAE*) and determination coefficient (R^2). The equations of the *RMSE*, *MAE* and R^2 are:

$$MSE = \frac{1}{N}\sum_{i=1}^{N}\left(x_i - y_i\right)^2 \tag{17}$$

$$RMSE = \sqrt{MSE} \tag{18}$$

$$MAE = \frac{1}{N}\sum_{i=1}^{n}\left|x_i - y_i\right| \tag{19}$$

$$R^2 = \frac{\left(\sum_{i=1}^{n}\left(x_i - \bar{x}\right)\left(y_i - \bar{y}\right)\right)^2}{\sum_{i=1}^{n}\left(x_i - \bar{x}\right)^2 \sum_{i=1}^{n}\left(y_i - \bar{y}\right)^2} \tag{19}$$

where N and y_i refer to number of data set and entropy parameter, respectively. *MSE* is mean square errors.

For estimating shear stress distribution of the streams, three different input combinations were used. The Pearson correlations between the inputs u_{ws}, S, y/T and output are 0.804, 0.772 and 0.031, respectively. The lowest linear relationship exists between the y/T and output and the u_{ws} has the highest correlation. According to the correlation values, u_{ws} seems to be the most effective variable on shear stress distribution. The optimal hidden node numbers were obtained for each ANN model by using simple trial and error method. The hidden node number tried for each ANN model ranges between 1 and 10. As an example, the variation of hidden node number *vs.* mean square error (*MSE*) in test stage for the ANN model with three inputs is illustrated in Fig. 6. The ANN models were trained by using Conjugate Gradient algorithm which is more powerful than the classical gradient descent technique. The sigmoid activation functions were used for the hidden and output nodes. The ANN training was stopped after 1000 iterations. Training and test results of the optimal ANN models are shown in Tab. 2 in respect of *RMSE*, *MAE* and R^2 statistics. The optimal hidden node numbers are also provided in the second column of this table. It is apparent from the table that the ANN model comprising three inputs corresponding to u_{ws}, S_{ws} and y/T, 6 hidden and 1 output nodes has the lowest *RMSE*, *MAE* and the highest R^2 both in training and test periods. From Tab. 2, it is clear that the accuracy of ANN

models significantly increases by adding input of y/T. For the ANFIS models, grid partition method was used by applying *genfis1* in MATLAB. Table 2 represents training and test results of the ANFIS model for each input combination. The second column of this table gives the optimal number of membership functions. It is clearly seen from Tab. 2 that the ANFIS model comprising 3 Gaussian membership functions for the inputs, u_{ws}, S and y/T outperforms the other ANFIS models for the both periods. Comparison of ANN and ANFIS models clearly indicates that the ANFIS models generally provide better shear stress estimates than the ANN models. The *RMSE*, *MAE* and R^2 statistics of the MLR models are also shown in Tab. 2. Second column of this table gives the regression coefficients of each model. The MLR model with the inputs of u_{ws}, S and y/T gives inferior results in relative to the ANN and ANFIS models. This implies the strong nonlinear relationship between u_{ws}, S and y/T inputs and shear stress distribution. The optimal ANFIS model respectively reduced the root mean square errors and mean absolute errors by 47% and 50% with respect to the optimal MLR model. t-statistics of each coefficient of the MLR model comprising three inputs calculated using Excel program are reported in Tab. 3. According to the table, all three coefficients seem to be significant at the 5% significance level.

Table 2. Training and test results of the ANN, ANFIS and MLR models in estimating shear stress distribution.

Input	Parameters	Training			Test		
		RMSE	*MAE*	R^2	*RMSE*	*MAE*	R^2
ANN							
u_{ws}	5	8.34	5.43	0.767	5.50	3.87	0.839
u_{ws} and S	1	8.78	5.63	0.742	5.06	3.23	0.875
u_{ws}, S and y/T	6	4.54	3.07	0.931	4.67	3.08	0.876
ANFIS							
u_{ws}	(gaussmf, 3)	8.99	5.76	0.730	5.14	3.57	0.849
u_{ws} and S	(gaussmf, 2)	8.79	5.71	0.742	5.08	3.05	0.869
u_{ws}, S and y/T	(gaussmf, 3)	4.51	3.24	0.932	3.85	2.85	0.921
MLR							
u_{ws}	(17.04)	12.40	9.42	0.613	8.50	7.60	0.837
u_{ws} and S	(5.0, 2430)	11.27	8.67	0.676	9.51	8.33	0.698
u_{ws}, S and y/T	(8.9, 2472, –10.5)	10.80	7.68	0.647	7.30	5.75	0.794

Table 3. t-statistics of the MLR coefficients for the u_{ws}, S and y/T inputs.

Coefficient	*t*-statistic	*P* value
8.9	3.18	0.001915
2472	5.17	0.000001
–10.5	–3.30	0.001824

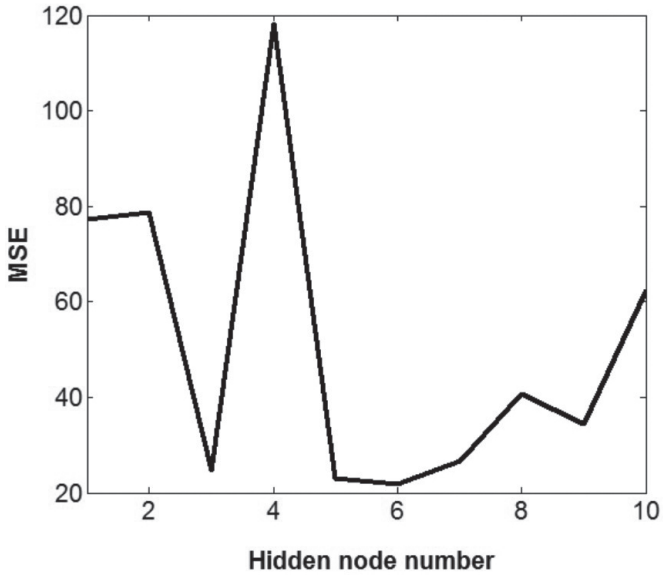

Figure 6. Variation of hidden node number vs *MSE* in test stage for the ANN model with three inputs.

The shear stress estimates of the ANN, ANFIS and MLR models in test period are illustrated in Fig. 7 for the test period. It is clear from the figure that the estimates obtained using ANFIS and ANN models are much closer to the corresponding measured shear stress values than those of the MLR model. Significantly under/over-estimations are clearly seen for the MLR.

Figure 8 demonstrates the test estimates of each model in the scatterplot form. It is clear from the figure that the shear stress estimates of the ANN and ANFIS models are closer to the corresponding measured values than those of the MLR model. The MLR having highly scattered estimates seems to be insufficient in estimating shear stress distribution of the natural streams. The ANFIS model performs better than the ANN model especially for the low and high shear stress values.

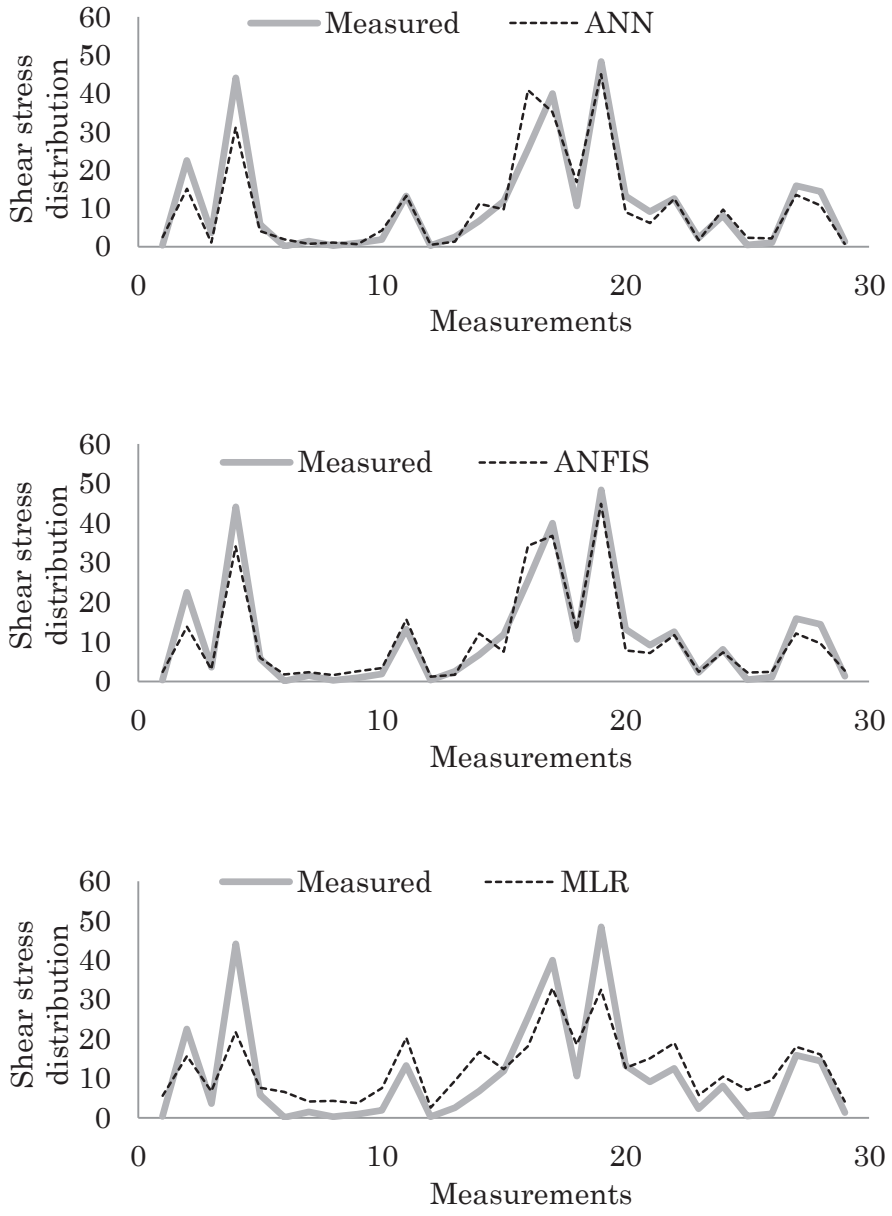

Figure 7. Time variation of the measured and estimated shear stress values by ANN, ANFIS and MLR models.

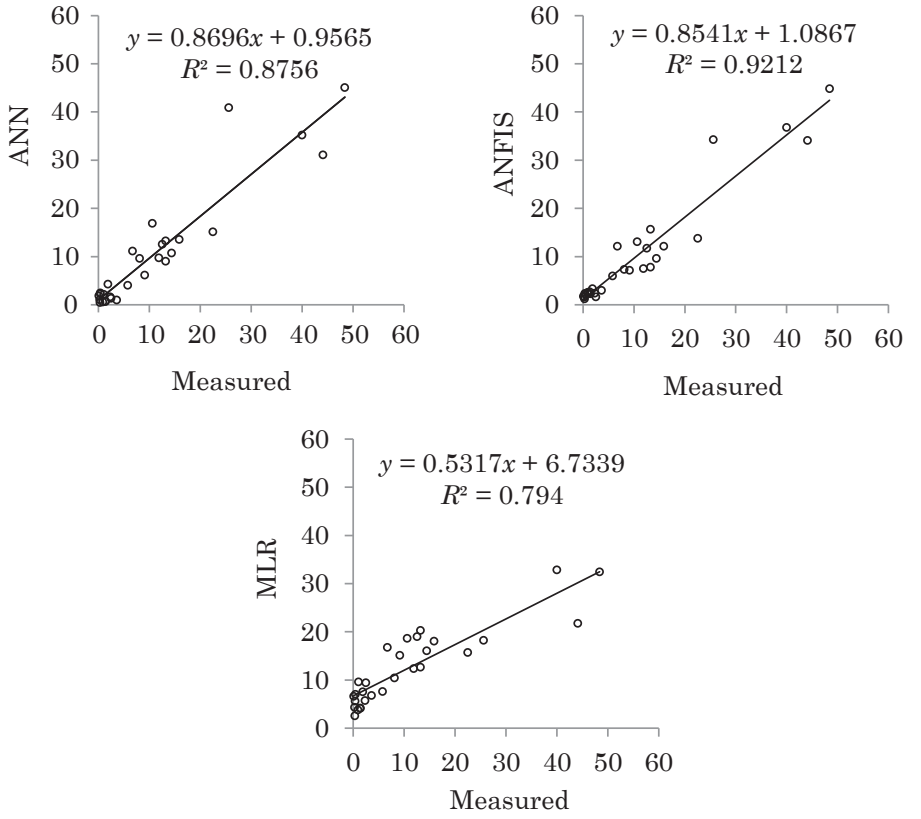

Figure 8. The scatterplots of the measured and estimated shear stress values by ANN, ANFIS and MLR models.

The results are tested by using one way ANOVA for verifying the robustness (the significance degree of differences between the model estimates and measured shear stress distribution) of the models. The test is set at a 95% significant level. Table 4 reports the test statistics. It is clear from the table that the ANFIS and ANN models yield small testing values with high significance levels. From Table 4, the ANFIS and ANN models seem to be more robust (the similarity between the measured entropy parameters and model estimates are significantly high) in shear stress estimation than the MLR model.

Table 4. ANOVA of ANFIS, ANN and MLR models in the test period.

Model	*F*-statistic	Resultant significance level
ANFIS(gaussmf, 3)	0.024	0.878
ANN(3,6,1)	0.020	0.889
MLR	0.302	0.585

6. Conclusion

This study investigated the accuracy of ANFIS and ANN methods for estimating shear stress distribution in streams. Overall 145 field data gauged from four different cross-sections at four sites on the Sarımsaklı and Sosun streams in Turkey were used. The water surface velocity $u_{ws,}$ water surface slope S and y/T were used as inputs to the ANFIS and ANN models for estimating shear stress distribution. The estimates obtained from the ANFIS and ANN models were compared with multiple-linear regression model. The results revealed that the ANFIS and ANN models performed much better than the MLR model in estimating shear stress distribution. The ANFIS was found to be slightly better than the ANN. The best ANFIS model was respectively reduced the root mean square errors and mean absolute errors by 47% and 50% with respect to the best MLR model. The study recommends that the ANFIS and ANN techniques can be successfully used for estimating shear stress distribution of the natural streams.

References

Ardiclioglu, M., Seckin, G. and Yurtal, R. (2006): Shear stress distributions along the cross section in smooth and rough open channel flows, *Kuwait J. Sci. Eng.*, **33**, 155–168.

Ardiclioglu, M., Genc, O., Kalin, L. and Agiralioglu, N. (2012): Investigation of flow properties in natural streams using the entropy concept, *Water Environ. J.*, **26**, 147–154, DOI: 10.1111/j.1747-6593.2011.00270.x.

Berlamont, J. E., Trouw, K. and Luyckx, G. (2003): Shear stress distribution in partially filled pipes, *J. Hydraul. Eng.-ASCE*, **129**, 697–705, DOI: 10.1061/(ASCE)0733-9429(2003)129:9(697).

Bilhan, O., Emiroglu, M. E. and Kisi, O. (2010): Application of two different neural network techniques to lateral outflow over rectangular side weirs located on a straight channel, *Adv. Eng. Softw.*, **41**, 831–837, DOI: 10.1016/j.advengsoft.2010.03.001.

Cacqueray, N., Hargreaves, D. M. and Morvan, H. P. (2009): A computational study of shear stress in smooth rectangular channels, *J. Hydraul. Res.*, **47**, 50–57, DOI: 10.3826/jhr.2009.3271.

Can, I., Tosunoglu, F. and Kahya, E. (2012): Daily streamflow modelling using autoregressive moving average and artificial neural networks models: case study of Çoruh basin, Turkey, *Water Environ. J.*, **26**, 567–576, DOI: 10.1111/j.1747-6593.2012.00337.x.

Christensen, B. and Fredsoe, J. (1998): *Bed shear stress distribution in straight channels with arbitrary cross section*, Progress Rep. 77. Dept. of Hydrodynamics and Water Resources, TU Denmark, Lyngby.

Cobaner, M., Seckin, G. and Kisi, O. (2008): Initial assessment of bridge backwater using artificial neural network approach, *Can. J. Civil Eng.*, **35**, 500–510.

Cobaner, M., Seckin, G., Seckin, N. and Yurtal, R. (2010): Boundary shear stress analysis in smooth rectangular channels and ducts using neural networks, *Water Environ. J.*, **24**, 133–139, DOI: 10.1111/j.1747-6593.2009.00165.x.

Dogan, E., Yuksel, I. and Kisi, O. (2007): Estimation of total sediment load concentration obtained by experimental study using artificial neural networks, *Environ. Fluid Mech.*, **7**, 271–288, DOI: 10.1007/s10652-007-9025-8.

Dursun, O. F., Kaya, N. and Firat, M. (2012): Estimating discharge coefficient of semi-elliptical side weir using ANFIS, *J. Hydrology*, **426–427**, 55–62, DOI: 10.1016/j.jhydrol.2012.01.010.

French, R. H. (1985): *Open-Channel Hydraulics*. McGraw-Hill Inc., New York, 620 pp.

Ghosh, S. N. and Roy, N. (1970): Boundary shear distribution in open channel flow, *J. Hydraulics Div. – Proc. ASCE*, **96**, 967–994.

Guven, A. (2011): A multi-output descriptive neural network for estimation of scour geometry downstream from hydraulic structures, *Adv. Eng. Softw.*, **42**, 85–93, DOI: 10.1016/j.advengsoft.2010.12.005.

Haykin, S. (2009): *Neural Networks and Learning Machines*. Prentice Hall, New Jersey, 906 pp.

Hicks, F. E., Jin, Y. C. and Steffler, P. M. (1990): Flow near sloped bank in curved channel, *J. Hydraul. Eng.-ASCE*, **116**, 55–70, DOI: 10.1061/(ASCE)0733-9429(1990)116:1(55).

Jang, J. S. R. (1993): ANFIS: Adaptive-network-based fuzzy inference system, *IEEE T. Syst. Man Cybern.*, **23**, 665–685, DOI: 10.1109/21.256541.

Jang, J. S. R., Sun, C. T. and Mizutani, E. (1997): *Neuro-Fuzzy and Soft Computing: A Computational Approach to Learning and Machine Intelligence*. Prentice Hall, New Jersey, 614 pp.

Khodashenas, S. R., Abderrezzak, K. K. and Paquier, A. (2008): Boundary shear stress in open channel flow: A comparison among six methods, *J. Hydraul. Res.*, **46**, 598–609, DOI: 10.3826/jhr.2008.3203.

Kisi, O. (2005): Suspended sediment estimation using neuro-fuzzy and neural network approaches, *Hydrol. Sci. J.*, **50**, 683–696, DOI: 10.1623/hysj.2005.50.4.683.

Kisi, O., Bilhan, O. and Emiroglu, M. E. (2013): ANFIS to estimate discharge capacity of rectangular side weir, *P. I. Civil Eng.-Wat. M.*, **166**, 479–487, DOI: 10.1680/wama.11.00095.

Knight, D. W. and Patel, H. S. (1985): Boundary shear in smooth rectangular ducts, *J. Hydraul. Eng.-ASCE*, **111**, 29–47, DOI: 10.1061/(ASCE)0733-9429(1985)111:1(29).

Knight, D. W., Yuen, K. W. H. and Alhamid, A. A. I. (1994): Boundary shears stress distributions in open channel flow, in: *Physical mechanisms of mixing and transport in the environment*, edited by Beven, K., Chatwin, P. and Millbank, J. Wiley, New York, 51–87.

Knight, D. W., Demetriou, J. D. and Hamed, M. E. (1984): Boundary shear in smooth rectangular channels, *J. Hydraul. Eng.-ASCE*, **110**, 405–422, DOI: 10.1061/(ASCE)0733-9429(1984)110:4(405).

Kocabas, U. and Ülker, S. (2006): Estimation of critical submergence for an intake in a stratified fluid media by neuro-fuzzy approach, *Environ. Fluid Mech.*, **6**, 489–500, DOI: 10.1007/s10652-006-9005-4.

Kocabas, F., Kisi, O. and Ardiclioglu, M. (2009): An artificial neural network model for prediction of critical submergence for an intake in a stratified fluid media, *Civ. Eng. Environ. Syst.*, **26**, 367–375, DOI: 10.1080/10286600802200130.

Lundgren, H. and Johnson, I. G. (1964): Shear and velocity distribution in shallow channels, *J. Hydr. Div.*, **90**, 1–21.

Mamak, M., Seckin, G., Cobaner, M. and Kisi, O. (2009): Bridge afflux analysis through arched bridge constrictions using artificial intelligence methods, *Civ. Eng. Environ. Syst.*, **26**, 279–793, DOI: 10.1080/10286600802151804.

Marsili-Libelli, S., Giusti, E. and Nocita, A. (2013): A new instream flow assessment method based on fuzzy habitat suitability and large scale river modelling, *Environ. Model. Softw.*, **41**, 27–38, DOI: 10.1016/j.envsoft.2012.10.005.

Mohammadi, M. and Knight, D. W. (2004): Boundary shear stress distribution in a V-shaped channel, in: *Hydraulics of Dams and River Structures*, edited by Yazdandoost, F. and Attari, J., Taylor & Francis Group, London, 401–410.

Rezaeianzadeh, M., Tabari, H., Yazdi, A. A., Isik, S. and Kalin, L. (2013): Flood flow forecasting using ANN, ANFIS and regression models, *Neural Comput. Applic.*, **25**, 25–37, DOI 10.1007/s00521-013-1443-6.

Riahi-Madvar, H., Ayyoubzadeh, S. A., Khadangi, E. and Ebadzadeh, M. H. (2009): An expert system for predicting longitudinal dispersion coefficient in natural streams by using ANFIS, *Exp. Syst. Appl.*, **36**, 8589–8596, DOI: 10.1016/j.eswa.2008.10.043.

Schlicting, H. (1987): *Boundary Layer Theory*. McGraw-Hill, New York, pp 525–529.

SonTek (2002): Flow Tracker Handheld ADV, Technical Document, available at ftp://ksh.fgg.uni-lj.si/students/podipl/merska_oprema/Flow_Tracker_Manual.pdf.

Tayfur, G., Nadiri, A. A. and Moghaddam, A. A. (2014): Supervised intelligent committee machine method for hydraulic conductivity estimation, *Water Resour. Manage.*, **28**, 1173–1184, DOI: 10.1007/s11269-014-0553-y.

Tracy, H. J. (1965): Turbulent flow in a three-dimensional channel, *J. Hydraulics Div.–Proc. ASCE*, **91(6)**, 9–35.

Wolfs, V. and Willems, P. (2013): A data driven approach using Takagi–Sugeno models for computationally efficient lumped floodplain modelling, *J. Hydrol.*, **503**, 222–232, DOI: 10.1016/j.jhydrol.2013.08.020.

Yang, S. Q. and Lim, S. Y. (2005): Boundary shear stress distributions in trapezoidal channels, *J. Hydraulic Res.*, **43**, 98–102, DOI: 10.1080/00221680509500114.

Yang, H. C. and Chang, F. J. (2005): Modelling combined open channel flow by artificial neural networks, *Hydro. Process*, **19**, 3747–3762, DOI: 10.1002/hyp.5858.

Yu, G. and Tan, S. K. (2007): Estimation of boundary shear stress distribution in open channels using flownet, *J. Hydraul. Res.*, **45**, 486–496, DOI: 10.1080/00221686.2007.9521783.

Zheng, Y. and Jin, Y. C. (1998): Boundary shear in rectangular ducts and channels, *J. Hydraul. Eng.-ASCE*, **124**, 86–89, DOI: 10.1061/(ASCE)0733-9429(1998)124:1(86).

SAŽETAK

Modeliranje razdiobe napetosti smicanja u prirodnim malim vodotocima metodama mekog računanja

Onur Genc, Ozgur Kisi i Mehmet Ardiclioglu

U ovoj studiji su za procjenu razdiobe napetosti smicanja u vodotocima korištene umjetne neuronske mreže (ANNs) i prilagodljivi neizraziti sustav zaključivanja (ANFIS). Metode su primijenjene na 145 nizova podataka prikupljenih na četiri različite postaje na vodotocima Sarimsakli i Sosun u Turskoj. Točnost primijenjenih modela uspoređena je s točnošću modela višestruke linearne regresije (MLR). Rezultati su pokazali da su oba modela (ANNs i ANFIS) bili bolji u modeliranju raspodjele napetosti smicanja od MLR modela. Pri korištenju ANFIS modela za procjenu raspodjele napetosti smicanja u testnom razdoblju srednje kvadratne pogreške (*RMSE*) i srednje apsolutne pogreške (*MAE*) su u odnosu na MLR model bile smanjene za 47%, odnosno 50%. Utvrđeno je da se za testno razdoblje najbolji ANFIS model, s $RMSE = 3{,}85$, $MAE = 2{,}85$ i koeficijentom određenosti $R^2 = 0.921$, pokazao superiornim u procjeni napetosti smicanja u odnosu na MLR model, s $RMSE = 7{,}30$, $MAE = 5{,}75$ i $R^2 = 0.794$.

Ključne riječi: ANN, ANFIS, linearna regresija, napetost smicanja, vodotok, turbulentni tok

Corresponding author's address: Ozgur Kisi, International Black Sea University, Tbilisi, Georgia; tel: +90 362 280 1081; email: okisi@ibsu.edu.ge